Mechatronic Design and Non-Commutative Behavior of a Cable-Driven, Underactuated Tensegrity Manipulator

Lauren Ervin, Harish Bezawada, and Vishesh Vikas

***Abstract*— Tensegrities synergistically combine elements of tension (elastic cable) and compression (rigid, curved-link) elements to achieve structural integrity, providing a high strength-to-mass ratio, compliance, and packability among other benefits. In space environments, lighter alternatives capable of predictable movement in different gravities are necessary. The Redundant, Extrinsically-Actuated Continuum Handling (REACH) robot is comprised of 12 homogeneous tensegrity primitives connected in series. A single tensegrity primitive consists of two semi-circular curved links held together by a continuous, elastic cable that is pre-stressed into 12 segments. The REACH robot is cable-driven via four motor tendon actuators (MTA) fixed at the base of the robot; this design provides balance between a reduction in control space (underactuation) while eliminating the need for counterweights. This unique design poses modeling and control challenges given (1) the entire manipulator is a closed chain, and (2) the MTA movement is non-linear, creating complex and sometimes unexpected behavior. A design framework that is tensegrity primitive invariant is shown, and the mechatronic system integration is laid out. In-line load cells display the non-linear movement resulting from preliminary tests of different input sequences.**

I. INTRODUCTION

Continuum robots provide balance between flexibility and dexterity, leading to increased capabilities in constrained environments [1]. To achieve adequate control that best utilizes the physical potential of these robots, models must be realized that accurately capture the movement. There is no one size fits all; material makeup, actuator choice, module connection points, and backbone composition all play roles in defining robot movement and reliability. Continuum robots come in many shapes with various actuation schemes [2]. This design choice can aid in appropriate applications, e.g. a snake-like robot with many repeating modules may choose an intrinsic design with actuators fixed along each module. Alternatively, to achieve a lighter-weight manipulator capable of lifting higher payloads for space applications, a designer might choose to control the device with remote actuators fixed to a base beyond the prototype in an extrinsic configuration. When actuator location is chosen, the placement of the tendon path can still greatly alter robot control [3].

*This work was supported in part by USDA/NIFA Award #2023-67022-40918. The material contained in this document is based upon work supported in part by a National Aeronautics and Space Administration (NASA) grant or cooperative agreement. Any opinions, findings, conclusions, or recommendations expressed in this material are those of the authors and do not necessarily reflect the views of NASA. This work was supported through a NASA grant awarded to the Alabama/NASA Space Grant Consortium.

[1]Lauren Ervin, Harish Bezawada, and Vishesh Vikas are with the Agile Robotics Lab, University of Alabama, Tuscaloosa, AL 35487, USA {lefaris and hbezawada}@crimson.ua.edu, vvikas@ua.edu

Developing a model is the next critical step [4]. The most widely used is Constant Curvature (CC) [5]–[7]. This heavily simplifies the Cosserat rod model [8], [9], making the assumption that robot movement consists of finite curved links that can be adequately described by curvature and angle of rotation. Variable Curvature (VC) [10] is another modeling technique that can account for changes in curvature by integrating functions, more accurately reflecting irregular curling. Both CC and VC rely on the presence of a predictable backbone which usually provides a combination of stability with flexibility during movement.

Tensegrities synergistically combine elements of tension (elastic cable) and compression (rigid, curved-link) elements to achieve structural integrity, providing a high strength-to-mass (S2M) ratio among other benefits. Consequently, they are lighter alternatives for interacting in unstructured environments. Due to their many advantages, researchers have garnered interest in creating continuum robot manipulators with tensegrity primitives. In fact, tensegrity manipulators exhibit a much higher S2M ratio than traditional robot manipulators. The traditional robot arm depicted in Fig. 1a contains multiple actuators fixed to the arm joints. This creates significant weight that hangs away from the base, limiting the additional payload that the robot arm is capable of lifting. Traditional robot manipulators can have a S2M ratio as low as 0.75:1 whereas preliminary tests with the REACH robot show >3:1.

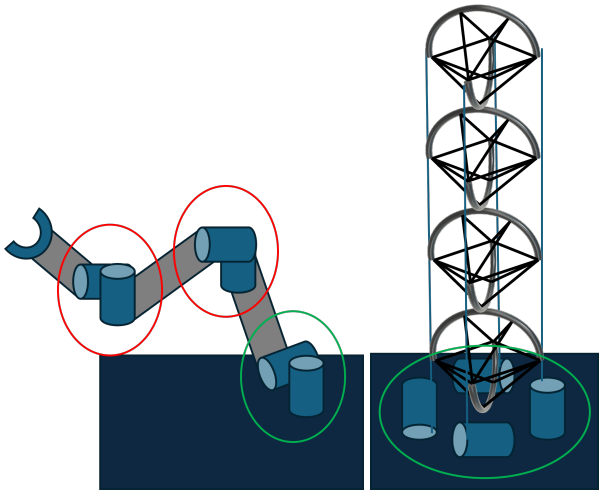

(a) Traditional arm (b) Tensegrity arm

Fig. 1: a) A rigid arm with motors attached throughout. b) A manipulator with motors fixed at the base with a lower CoM.

Contributions. This work presents a design methodology for a Redundant, Extrinsically-Actuated Continuum Handling (REACH) robot. By embedding the motor actuators within the base, the REACH robot is 1) capable of dynamic manipulation without the need for counterweights, and 2) exhibits a high strength-to-mass (S2M) ratio. The use of only four motor-tendon actuators (MTAs) reduces the control space due to the finite number of driving cables. The REACH robot is fabricated by connecting multiple tensegrity primitives together in series, and this provides both compliant and modular properties where length can vary by adding or subtracting modules and shape/movement can change by swapping in a different tensegrity primitive. A physical prototype expresses the non-linear nature of the system with in-line tension data from preliminary experimentation.

II. MECHATRONIC SYSTEM DESIGN

A. Design Requirements

The tensegrity continuum manipulator should exhibit the following requirements.

1) *Lightweight:* The weight of the manipulator should have a ≥ 2 S2M ratio, e.g. if the manipulator weighs 4kg, it should be able to lift at least 8kg.
2) *Compliant:* The manipulator should be able to interact with the environment without being damaged. Additionally, unintended interaction should not result in drastic changes in end effector position.
3) *Modular:* The individual tensegrity primitives should be both easy to remove/add for length varying, and invariant to the specific primitive; swapping in a different primitive such as an icosahedron should have minor impacts on overall locomotion patterns that are understood in modeling.

B. Manipulator Design

The continuum manipulator consists of 12 identical tensegrity primitives connected in series. The unique design of the primitive in Fig. 2 poses static and dynamic modeling challenges. Each of the tensegrity primitives are closed chains. Although the full manipulator may at first appear to be an open chain, it is a connection of closed chains meaning that when a driving cable actuates, movement of one primitive affects the shape and orientation of the other 11. Additionally, the system is underactuated and thus the MTA movement is non-linear, creating complex behavior. Two examples of the non-linear behavior is shown in Sec. III.

C. Platform Design

Two curved arcs comprising a primitive were water jet out of aluminum and held together with a continuous Nylon elastic cable. The primitives were connected in series through connection points at the base of each arc. The continuum manipulator is cable-driven with four MTA consisting of E30-150-24-PR32 brushed DC motors with 1:32 planetary gear boxes and optical encoders. The manipulator is fixed to a wheeled platform fabricated primarily out of 80/20 and driven with E30-150-24 brushed DC motors with 1:16 planetary gear boxes. The chassis houses the four MTAs and all associated electronics enclosed in acrylic sheets to protect from outside elements.

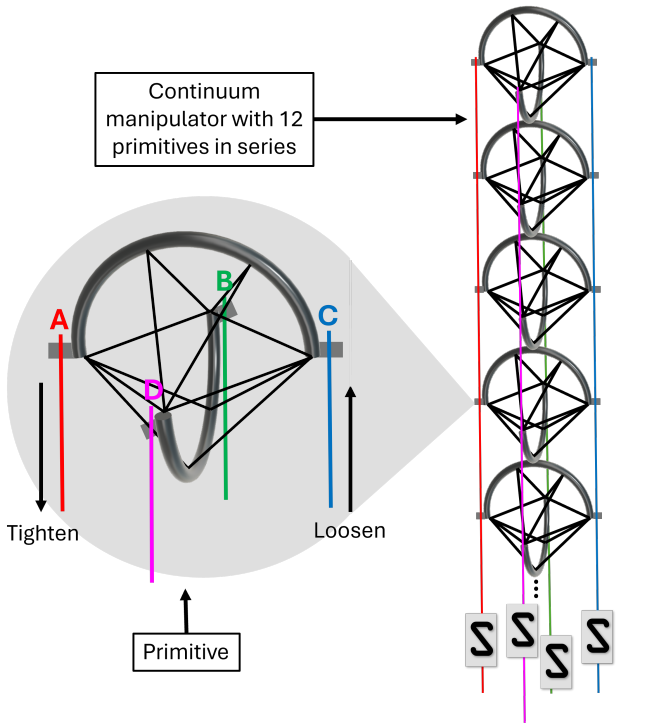

Fig. 2: The REACH robot containing 12 individual primitives connected in series. The tensegrity continuum manipulator is controlled via four tendon cables running in the cardinal directions down its body. Additionally, four in-line load cells measure cable tension.

D. Electronics

Data is collected from four S-type FRC4163_0 load cells and three to seven BNO085 IMUs. The 9-axis IMUs measure the orientation and acceleration at different points along the manipulator from tip to base, and the load cells measure the in-line tension along the four driving cables. The IMU data is read via an I2C MUX, and the load cell data is read from a high-frequency DAQ system. A data PCB whose schematic is shown in Fig. 3 facilitates all data collection from the system. The PCB then connects to a Jetson Orin Nano which coordinates all motor control of the system.

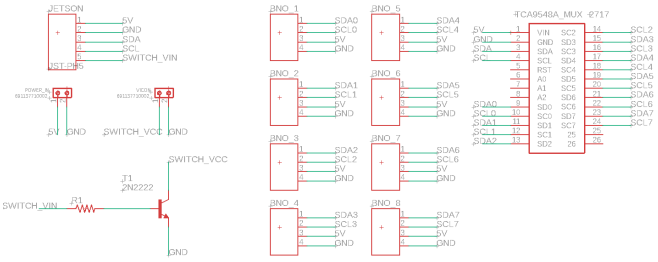

Fig. 3: Data PCB schematic.

Power is delivered to all system components from either a 24V 42A DC PSU for wall power during in-lab experiments or a 22.2V 10Ah LiPo for tetherless capabilities during in-field tests. Power diodes and fuses are connected to the power input to prevent excessive current draw. Pull-up resistors are used to interface with the encoders and filter capacitors are used to reduce noise in the system. Additionally, RoboClaw motor controllers enable further current limiting to each DC motor. A voltage regulator drops VCC to 5V for all logic components on the data PCB. Finally, an E-stop is connected to increase the safety of the system.

III. NON-COMMUTATIVE BEHAVIOR

The continuum manipulator exhibits non-commutative behavior in multiple ways. We are specifically interested in how order of operations and reversed order commands affects end effector position. Two examples exhibiting this non-linear behavior are shown.

A. *Opposite Commands in Reverse Order are Not Equivalent*

For a set of two input sequences with the exact same set of motor commands going forwards and then backwards, the backwards sequence will not always end in the same position that the forward sequence started in. A forward sequence starts with Fig. 4a, ending with Fig. 4b. Then, the same path is traveled in reverse order, starting with Fig. 4c and ending with Fig. 4d. One would expect the robot orientations in Fig. 4a and Fig. 4d to match, but they do not always, as is seen in Fig. 4.

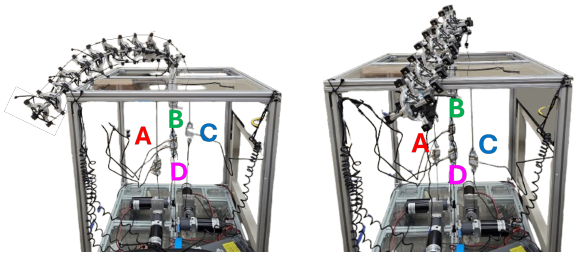

(a) Forward path starting (b) Forward path ending

(c) Reverse path starting (d) Reverse path ending

Fig. 4: REACH robot following a forward path in a) and b), then the same path reversed in c) and d). If the cable-driven movements were linear, the starting position of the forward path a) and the ending position of the reversed path d) would match.

The variation in robot position is also seen in the in-line load cell values. In Fig. 5, the first path traveling from Fig. 4a to Fig. 4b is shown with the solid forward lines. Similarly, the reverse path traveling from Fig. 4c to Fig. 4d is shown with the dashed reverse lines. The solid and dashed lines should be mirrored, but there is a large magnitude offset present in all four load cells during the two paths. Finally, the starting dots of the forward path and the ending dots of the reversed path do not exactly match, especially with load cell 4. Although some variance is expected due to noise error, that alone is not a suitable explanation for load cell 4.

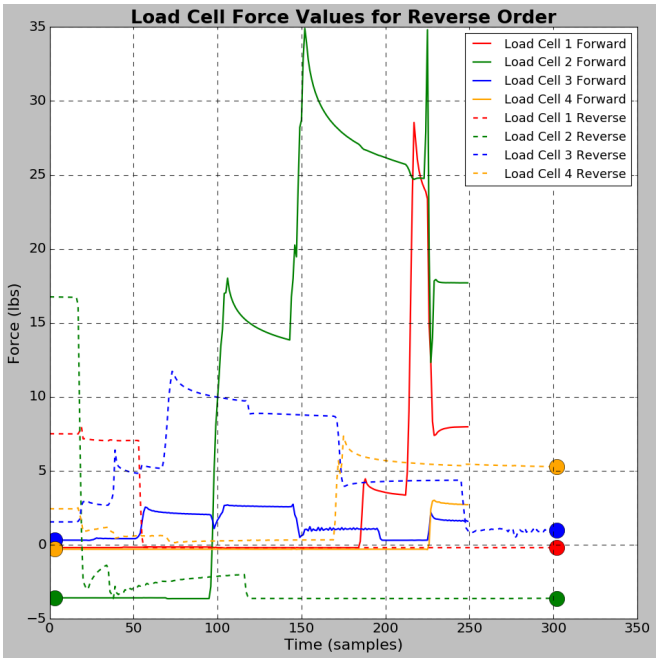

Fig. 5: The load cell values throughout the forward and reverse paths taken in Fig. 4. The starting load cell forces of the forward path and the ending load cell forces of the reversed path are both indicated with markers.

B. *Different Order, Different Output*

When starting in the same configuration, the same set of commands performed in a different order results in two unique endpoints. A forward sequence starts with Fig. 6a and ends with Fig. 6b. Then, the same set of motor commands in an altered order start with Fig. 6c and end with Fig. 6d. One would expect the ending robot orientations of Fig. 6b and Fig. 6d to match.

Similar variation is seen with the in-line load cell values. In Fig. 7, the first path from the set of motor commands travels from Fig. 6a to Fig. 6b and is shown with the solid order 1 lines. The second, slightly altered path of the same set of motor commands traveling from Fig. 6c to Fig. 6d is shown with the dashed order 2 lines. The solid and dashed lines will not match exactly since the path traveled is altered. However, the magnitude of the ending dots of both paths should match. The ending values for load cells 3 and 4 match, load cell 1 is on the same order of magnitude in both paths, and load cell 2 varies by over three times.

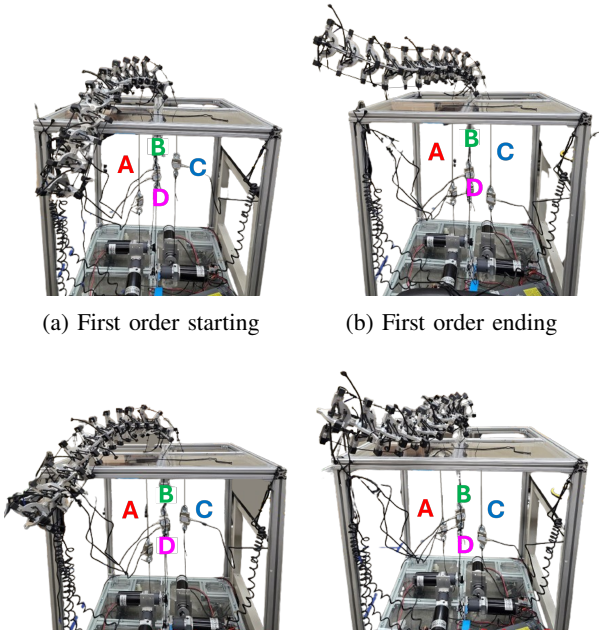

(a) First order starting (b) First order ending

(c) Different order starting (d) Different order ending

Fig. 6: REACH robot following the same set of motor commands in two slightly different orders. A set of motor commands is followed in a) and b), then the same set of motor commands in a slightly different order is followed in c) and d). Again, if the cable-driven movements were linear, one would expect the ending position of the first and slightly different order b) and d) to match.

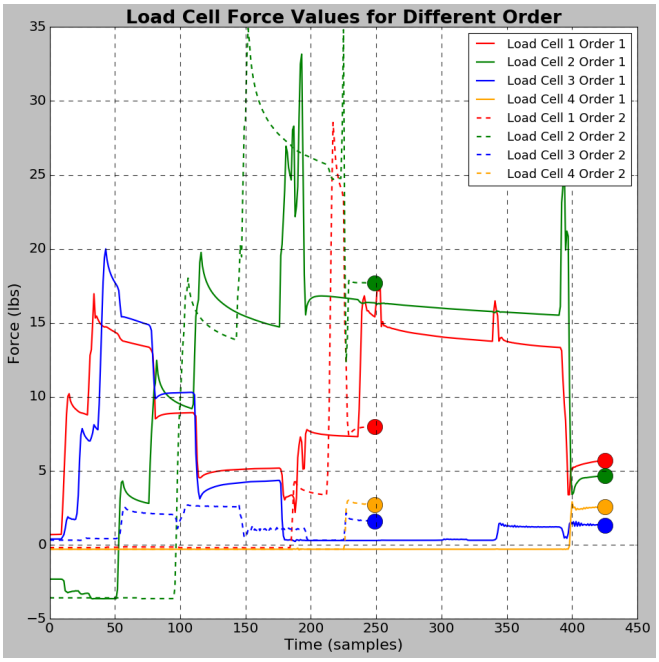

Fig. 7: The load cell values throughout the same set of motor commands in two slightly different orders shown in Fig. 6. The ending load cell forces of the two paths are both indicated with markers.

IV. CONCLUSION

The Redundant, Extrinsically-Actuated Continuum Handling (REACH) robot is presented. This cable-driven tensegrity manipulator is well suited for applications in space where compliant robots unaffected by changes in gravity can maintain a high strength-to-mass ratio for effective interaction with the environment. Additionally, the manipulator has all four MTAs fixed at the base of the robot, further increasing the stability of the system while enabling a reduction in the control space. The mechatronic, tensegrity primitive invariant design is laid out with details for the integration of the manipulator, platform, and electronics. Finally, preliminary input path tests show the non-linear behavior present within the system due to the underactuation. Future works include further development of a dynamic modeling framework to implement control with a Newton-Euler algorithm paired with sensor fusion feedback from the in-line load cells and IMUs to help correct any persisting non-linearities.

REFERENCES

[1] I. D. Walker, "Continuous backbone "continuum" robot manipulators," *International Scholarly Research Notices*, vol. 2013, no. 1, p. 726506, 2013.

[2] G. Robinson and J. Davies, "Continuum robots - a state of the art," in *Proceedings 1999 IEEE International Conference on Robotics and Automation (Cat. No.99CH36288C)*, vol. 4, pp. 2849–2854 vol.4, May 1999. ISSN: 1050-4729.

[3] H. Bai, B. G. Lee, G. Yang, W. Shen, S. Qian, H. Zhang, J. Zhou, Z. Fang, T. Zheng, S. Yang, L. Huang, and B. Yu, "Unlocking the Potential of Cable-Driven Continuum Robots: A Comprehensive Review and Future Directions," *Actuators*, vol. 13, p. 52, Feb. 2024. Number: 2 Publisher: Multidisciplinary Digital Publishing Institute.

[4] P. Rao, Q. Peyron, S. Lilge, and J. Burgner-Kahrs, "How to Model Tendon-Driven Continuum Robots and Benchmark Modelling Performance," *Frontiers in Robotics and AI*, vol. 7, Feb. 2021. Publisher: Frontiers.

[5] B. Jones and I. Walker, "Kinematics for multisection continuum robots," *IEEE Transactions on Robotics*, vol. 22, pp. 43–55, Feb. 2006. Conference Name: IEEE Transactions on Robotics.

[6] S. B. Andersson, "Discretization of a Continuous Curve," *IEEE Transactions on Robotics*, vol. 24, pp. 456–461, Apr. 2008. Conference Name: IEEE Transactions on Robotics.

[7] R. J. Webster and B. A. Jones, "Design and Kinematic Modeling of Constant Curvature Continuum Robots: A Review," *The International Journal of Robotics Research*, vol. 29, pp. 1661–1683, Nov. 2010. Publisher: SAGE Publications Ltd STM.

[8] S. S. Antman, *Nonlinear Problems of Elasticity*, vol. 107 of *Applied Mathematical Sciences*. New York, NY: Springer, 1995.

[9] D. Trivedi, A. Lotfi, and C. D. Rahn, "Geometrically Exact Models for Soft Robotic Manipulators," *IEEE Transactions on Robotics*, vol. 24, pp. 773–780, Aug. 2008. Conference Name: IEEE Transactions on Robotics.

[10] J. S. Kim and G. S. Chirikjian, "Conformational Analysis of Stiff Chiral Polymers with End-Constraints," *Molecular simulation*, vol. 32, no. 14, pp. 1139–1154, 2006.